Simultaneous Estimation of Primary Voltage and Mutual Inductance Based on Secondary-Side Information in Wireless Power Transfer Systems

Katsuhiro Hata, Takehiro Imura, and Yoichi Hori
The University of Tokyo
5–1–5, Kashiwanoha, Kashiwa, Chiba, 277–8561, Japan
Phone: +81-4-7136-3881, Fax: +81-4-7136-3881
Email: hata@hflab.k.u-tokyo.ac.jp, imura@hori.k.u-toyko.ac.jp, hori@k.u-tokyo.ac.jp

***Abstract*—A dynamic wireless power transfer (WPT) system for electric vehicles (EVs) has gathered attention and been expected to extend the limited driving range of EVs. Previous research has proposed secondary-side-only power and efficiency control to simplify the road-side facilities, which are installed over long distances. Although the primary voltage and the mutual inductance between the transmitter and receiver have to be given or estimated in the control, multi-parameter estimation from the secondary side without signal communication remains unrealized. This paper proposes a simultaneous estimation method of the primary voltage and the mutual inductance using only secondary-side information. The simulations and the experiments show that the proposed method is effective for secondary-side control.**

***Keywords*—Magnetic resonance, parameter estimation, electric vehicles, AC-DC power converters, power control.**

I. Introduction

Wireless power transfer (WPT) has received attention in recent years for industrial and automotive applications [1]–[3]. Eliminating the use of wiring can mitigate complicated charging operations and reduce the risk of accidents such as electrical shock, cable disconnection, and so on. An efficient power transmission and a stable supply of energy are important issues for implementing an actual WPT system.

WPT via magnetic resonance coupling provides a highly efficient mid-range transmission and robustness to misalignment [4]. These characteristics are suitable for dynamic charging of electric vehicles (EVs) and it can extend the limited driving range of EVs [1], [2]. Its road-side facilities, which are installed over long distances, should be simplified and secondary-side control is desired. If the primary voltage and the mutual inductance between the transmitter and the receiver are given or estimated, power and efficiency control can be achieved on the secondary side [5], [6]. Although multi-parameter estimation using primary-side information [7] and coupling coefficient estimation from either side [8] have been proposed, multi-parameter estimation from the secondary side without signal communication remains unrealized.

This paper proposes a simultaneous estimation method of the primary voltage and the mutual inductance using only secondary-side information. The effectiveness of the proposed method is verified by the simulations and the experiments.

II. System Structure

A. Circuit Structure

Fig. 1 shows the circuit diagram of the WPT system. The power source consists of the voltage source V_S and the full-bridge inverter, which is operated at the resonance frequency of the transmitter and the receiver. As this paper uses a series-series (SS) compensated circuit topology, the operating angular frequency ω_0 is given as follows:

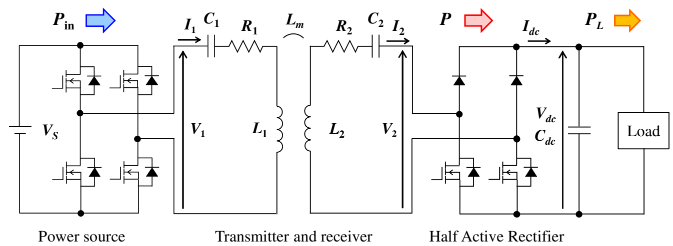

Fig. 1. Circuit diagram of the wireless power transfer system.

$$\omega_0 = \frac{1}{\sqrt{L_1 C_1}} = \frac{1}{\sqrt{L_2 C_2}}. \tag{1}$$

Half Active Rectifier (HAR) is used as an AC-DC converter and composed of the upper arm diodes and the lower arm MOSFETs. The load includes batteries, motors, other power converters, and so on. Although a constant power load can be available, this paper assumes that a constant voltage load is connected and its amplitude is determined by the battery voltage or controlled by other power converters.

B. Secondary-Side Control by HAR

HAR is operated by two different modes, which are shown in Fig. 2. During the rectification mode, the MOSFETs are maintained in the off-state and HAR is operated as the diode rectifier. Then, the transmitting power P flows to the DC link capacitor and the load. On the other hand, the short mode is worked by turning on the MOSFETs and the receiver is shorted. As a result, P is cut-off and the load power P_L is supplied by the DC link capacitor.

By combining the two operation modes, power control can be achieved on the secondary side [3]. Furthermore, if an additional DC-DC converter is put in the secondary side of the system, the desired power and maximum power transmitting efficiency can be achieved simultaneously [5], [6]. However, in order to obtain the reference value of the control, the primary voltage and the mutual inductance have to be given or estimated. In this paper, the two different operation modes of HAR are focused and a simultaneous estimation method of the primary voltage and the mutual inductance is proposed.

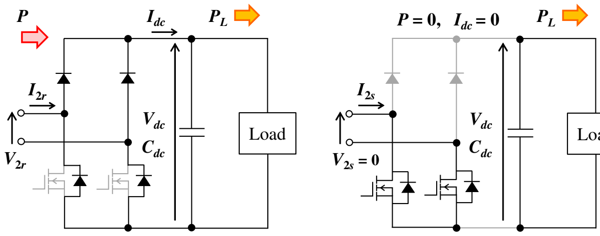

(a) Rectification mode. (b) Short mode.

Fig. 2. Operation modes of Half Active Rectifier.

TABLE I. SPECIFICATIONS OF COILS.

	Primary side	Secondary side
Resistance R_1, R_2	1.19 Ω	1.23 Ω
Inductance L_1, L_2	617 μH	617 μH
Capacitance C_1, C_2	4000 pF	4000 pF
Resonance frequency f_1, f_2	101.3 kHz	101.3 kHz
Mutual inductance L_m	77.8 μH (Gap: 200 mm)	
	37.3 μH (Gap: 300 mm)	
Coupling coefficient k	0.126 (Gap: 200 mm)	
	0.060 (Gap: 300 mm)	
Outer diameter	440 mm	
Number of turns	50 turns	

C. Experimental Setup

In order to verify the effectiveness of the proposed method, experimental equipment are implemented. Coils and power converters are shown in Fig. 3 and specifications of coils are expressed in TABLE I. The power source consists of a DC power supply (ZX-400LA, TAKASAGO) and the full-bridge inverter, which provides the transmitter with a square wave voltage. The inverter and the HAR are controlled by a DSP (PE-PRO/F28335A, Myway) and the load is simulated by an electronic load (PLZ1004W, KIKUSUI). The RMS secondary current I_2 is used for the estimation method and measured by a mixed signal oscilloscope (MSO3034, Tektronix).

III. PROPOSED ESTIMATION METHOD

A. Secondary Current

If a voltage source is used in the SS circuit topology of WPT via magnetic resonance coupling, the RMS secondary current I_2 can be approximated as follows:

$$I_2 \simeq \frac{\omega_0 L_m V_{11} - R_1 V_{21}}{R_1 R_2 + (\omega_0 L_m)^2} = \frac{2\sqrt{2}}{\pi} \frac{\omega_0 L_m V_1 - R_1 V_2}{R_1 R_2 + (\omega_0 L_m)^2} \quad (2)$$

where V_{11} and V_{21} are the RMS values of the fundamental primary and secondary voltages. From Fourier series expansion, they can be calculated by the RMS values of the primary voltage V_1 and the secondary voltage V_2. Assuming that the secondary voltage becomes a square wave and the voltage drop of the diodes are negligible, V_2 equals to the amplitude of the DC link voltage V_{dc}.

Fig. 4 shows experimental results of the RMS secondary current I_2. As the measured values and the calculated values are closely matched, eq. (2) can be applied to the estimation method. Since V_2 and I_2 can be obtained during each operation modes of HAR and eq. (2) is a linear function of V_2, any two parameters can be estimated simultaneously.

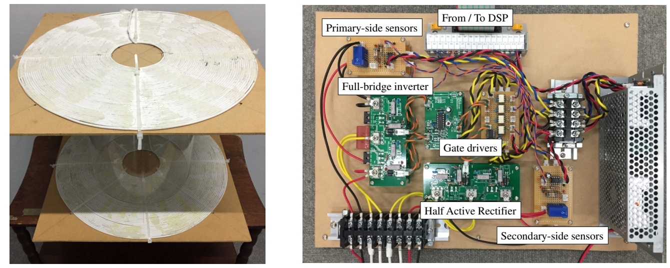

(a) Coils. (b) Power converters.

Fig. 3. Experimental equipment.

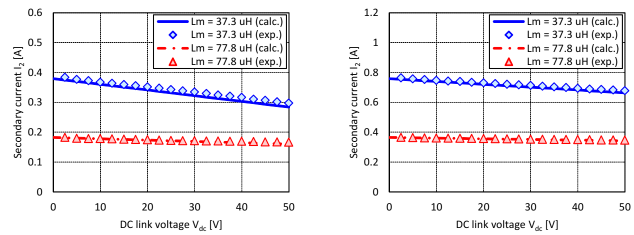

(a) $V_1 = 10$ V. (b) $V_1 = 20$ V.

Fig. 4. Experimental results of the RMS secondary current I_2.

B. Simultaneous Estimation of the Primary Voltage and Mutual Inductance

For distinguishing between unknown parameters and measurable parameters, eq. (2) is transformed as follows:

$$\omega_0 L_m V_{11} - I_2(\omega_0 L_m)^2 = R_1(V_{21} + R_2 I_2). \quad (3)$$

Then, the estimation equation is given as follows:

$$x_1 - I_2 x_2 = R_1(V_{21} + R_2 I_2) \quad (4)$$

$$\boldsymbol{x} = \begin{bmatrix} x_1 & x_2 \end{bmatrix}^T := \begin{bmatrix} \omega_0 L_m V_{11} & (\omega_0 L_m)^2 \end{bmatrix}^T. \quad (5)$$

Therefore, estimated parameter $\hat{\boldsymbol{x}}$ can be obtained as follows:

$$\hat{\boldsymbol{x}} = \begin{bmatrix} \hat{x}_1 & \hat{x}_2 \end{bmatrix}^T = \boldsymbol{A}^{-1}\boldsymbol{b} \quad (6)$$

$$\boldsymbol{A} := \begin{bmatrix} 1 & -I_{2r} \\ 1 & -I_{2s} \end{bmatrix}, \ \boldsymbol{b} := \begin{bmatrix} R_1(V_{21r} + R_2 I_{2r}) \\ R_1(V_{21s} + R_2 I_{2s}) \end{bmatrix}$$

where I_{2r}, V_{21r}, I_{2s}, and V_{21s} are measured values of I_2 and V_{21} during the rectification mode and during the short mode.

Assuming that the secondary voltage is a square wave and the voltage drop of the MOSFETs is negligible, V_{21r} and V_{21s} are calculated as follows:

$$V_{21r} = \frac{2\sqrt{2}}{\pi} V_{2r} = \frac{2\sqrt{2}}{\pi}(V_{dc} + 2V_f) \quad (7)$$

$$V_{21s} = \frac{2\sqrt{2}}{\pi} V_{2s} = 0 \quad (8)$$

where V_f is the forward voltage of the diodes. From eq. (5) and eq. (6), the estimated values of the mutual inductance $\hat{L}_m$ and the RMS primary voltage $\hat{V}_1$ are obtained as follows:

$$\hat{L}_m = \frac{1}{\omega_0}\sqrt{\hat{x}_2} \quad (9)$$

$$\hat{V}_1 = \frac{\pi}{2\sqrt{2}}\hat{V}_{11} = \frac{\pi}{2\sqrt{2}}\frac{\hat{x}_1}{\omega_0 \hat{L}_m}. \quad (10)$$

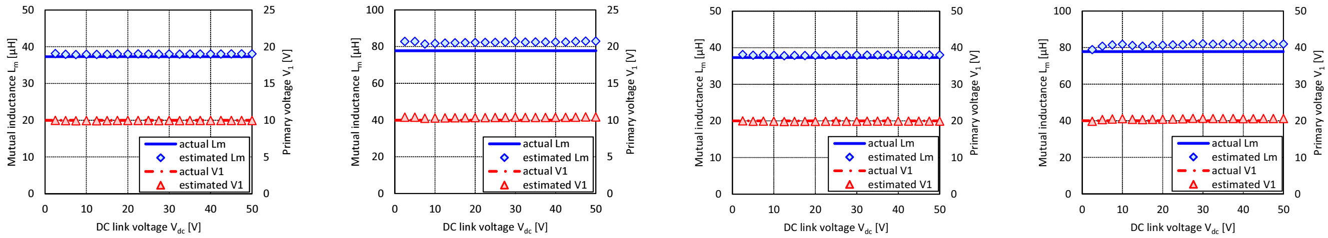

(a) $V_1 = 10$ V, $L_m = 37.3$ μH. (b) $V_1 = 10$ V, $L_m = 77.8$ μH. (c) $V_1 = 20$ V, $L_m = 37.3$ μH. (d) $V_1 = 20$ V, $L_m = 77.8$ μH.

Fig. 5. Simulation results of V_1 and L_m estimation.

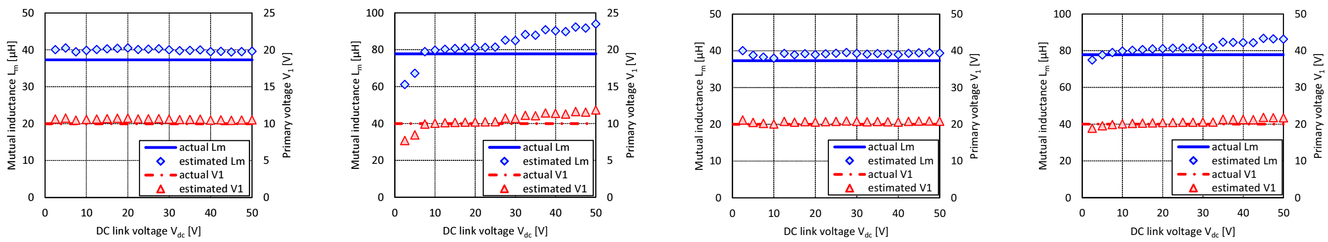

(a) $V_1 = 10$ V, $L_m = 37.3$ μH. (b) $V_1 = 10$ V, $L_m = 77.8$ μH. (c) $V_1 = 20$ V, $L_m = 37.3$ μH. (d) $V_1 = 20$ V, $L_m = 77.8$ μH.

Fig. 6. Experimental results of V_1 and L_m estimation.

IV. Simulation and Experiment

Simulations were performed by MATLAB Simlink SimPowerSystems. The circuit configuration is shown in Fig. 1. The load was assumed to be a constant voltage and its amplitude V_{dc} was gradually increased in 2.5 V increments from 2.5 V to 50 V during the simulation and the experiment. V_1 and L_m were estimated in each conditions.

Simulation results of V_1 and L_m estimation are shown in Fig. 5 and indicate that the proposed method can obtain the estimated values adequately. Although the estimated values are slightly larger than the actual values in Fig. 5 (b) and (d), these estimated errors are acceptable for secondary-side control.

Fig. 6 shows experimental results of V_1 and L_m estimation. In comparison with simulation results, the accuracy of the estimated values is reduced. Especially, Fig. 6 (b) is the worst case due to a low V_1 and a high L_m. This is because the difference of I_2 between the rectification mode and the short mode is quite small. As a result, a resolution capability of the current measurement greatly affects the estimation accuracy. However, Fig. 6 (c) shows that the estimated values accord closely with the actual values. Therefore, the proposed method is more effective in high power and low coupling application such as dynamic charging for EVs.

V. Conclusion

This paper proposed a simultaneous estimation method of the primary voltage and the mutual inductance based on the different operation modes of HAR. The simulation and experimental results demonstrated that the proposed method is effective for secondary-side control.

In future works, the proposed method is analyzed from the perspective of dynamic characteristics for secondary-side control and applied to dynamic WPT systems for EVs.

Acknowledgments

This work was partly supported by JSPS KAKENHI Grant Number 25709020 and 15H02232.

References

[1] G. A. Covic and J. T. Boys, "Modern trends in inductive power transfer for transportation application," *IEEE J. Emerg. Sel. Topics Power Electron.*, vol. 1, no.1, pp. 28–41, Mar. 2013.

[2] J. Shin, S. Shin, Y. Kim, S. Ahn, S. Lee, G. Jung, S. Jeon, and D. Cho, "Design and implementation of shaped magnetic-resonance-based wireless power transfer system for roadway-powered moving electric vehicles," *IEEE Trans. Ind. Electron.*, vol. 61, no. 3, pp. 1179–1192, Mar. 2014.

[3] D. Gunji, T. Imura, and H. Fujimoto, "Basic study of transmitting power control method without signal communication for wireless in-wheel motor via magnetic resonance coupling," in *Proc. IEEE/IES Int. Conf. Mech.*, 2015, pp. 313–318.

[4] A. Kurs, A. Karalis, R. Moffatt, J. D. Joannopoulos, P. Fisher, and M. Soljacic, "Wireless power transfer via strongly coupled magnetic resonance," *Science Express on 7 June 2007*, vol. 317, no. 5834, pp. 83–86, Jun. 2007.

[5] G. Lovison, M. Sato, T. Imura, and Y. Hori, "Secondary-side-only simultaneous power and efficiency control for two converters in wireless power transfer system," in *Proc. IEEE Ind. Electron. Soc. Conf.*, 2015, pp. 4824–4829.

[6] K. Hata, T. Imura, and Y. Hori, "Dynamic wireless power transfer system for electric vehicle to simplify ground facilities - power control and efficiency maximization on the secondary side -," in *Proc. IEEE Appl. Power Electron. Conf. Expo.*, 2016, pp. 1731–1736.

[7] J. P. W. Chow and H. S. H. Chung, "Use of primary-side information to perform online estimation of the secondary-side information and mutual inductance in wireless inductive link," in *Proc. IEEE Appl. Power Electron. Conf. Expo.*, 2015, pp. 2648–2655.

[8] V. Jiwariyavej, T. Imura, and Y. Hori, "Coupling coefficients estimation of wireless power transfer system via magnetic resonance coupling using information from either side of the system," *IEEE J. Emerg. Sel. Topics Power Electron.*, vol. 3, no.1, pp. 191–200, Mar. 2015.